JET–P(98)41

X Litaudon et al

Electron and Ion Internal Transport Barriers in Tore Supra and JET

JET–P(98)41

Electron and Ion Internal Transport Barriers in Tore Supra and JET

X Litaudon[1], T Aniel[1], Y Baranov, D Bartlett, A Bécoulet[1], C Challis, G A Cottrell, A Ekedahl[2], M Erba[1], L-G Eriksson, C Gormezano, G T Hoang[1], G Huysmans, F Imbeaux[1], E Joffrin[1], M Mantsinen[3], V Parail, Y Peysson[1], F Rochard, P Schild, A Sips, F X Söldner, B Tubbing, I Voitsekhovitch[4], D Ward, W Zwingmann.

JET Joint Undertaking, Abingdon, Oxfordshire, OX14 3EA,
[1]Association Euratom-CEA, Département de Recherches sur la Fusion Controlée, Certre d'Etudes de Cadarache, F-13108 Saint Paul-Lez-Durance Cedex, France.
[2]Chalmers University of Technology, Gothenberg, Sweden.
[3]Association Euratom-TEKES, Helsinki University of Technology, Finland.
[4]Université de Provence, Mrseille, France.

Preprint of a Paper to be submitted for publication in
Plasma Physics and Controlled Fusion

December 1998

ABSTRACT.

Formation of core regions in Tore Supra and JET tokamaks with reduced transport coefficients is reported. Characteristics of the enhanced confinement regions and the physics process involved in their formation and maintenance should be considered separately when the electron or ion components are predominantly heated.

In Tore Supra and JET, central electron temperature transitions are observed by injecting Lower Hybrid waves at modest power levels during the current ramp-up phase of the discharges. Transport analyses stress the importance of the low magnetic shear in the core to explain the anomalous electron transport reduction.

With high power dominant ion heating schemes in JET (neutral beam injection and ion cyclotron resonance heating), internal transport barriers have been obtained in plasmas fuelled with a mixture of deuterium-tritium (D-T) ions leading to a successful production of fusion power (8.2 MW) in this regime. Similar additional power levels to those applied in pure deuterium (D-D) plasmas are required to establish internal transport barriers in D-T plasmas. In D-D and D-T plasmas, ion thermal diffusivities are reduced close to their neoclassical levels in the plasma core and electron thermal diffusivities decrease by one order of magnitude at mid-plasma radius. The combined role of magnetic shear and ExB velocity shear can explain the formation and evolution of plasma core regions with low energy transport coefficients.

1. INTRODUCTION

Significant progress have been achieved over the past decade in reducing anomalous energy transport in tokamak plasmas. In addition to the well known improved confinement regime with a transport barrier at the plasma edge (H-mode) (e.g. Wagner et al 1982), recent experiments performed in most tokamaks have shown that spontaneous reduction in anomalous transport can also occur inside the plasma core to form an Internal Transport Barrier, ITB (e.g. DIII-D : Strait et al 1995; JT60-U : Ishida et al 1997; JET : JET team 1997, Söldner et al 1997; TFTR : Levinton et al 1995; Tore Supra, Moreau et al 1993). Regimes with ITBs are promising for high performance steady-state tokamak operation since they offer the opportunity i) to separate the high core reactivity region from the plasma edge, ii) to increase the fraction of self-generated bootstrap current (Kikuchi 1990, Jacquinot et al 1993, Bécoulet et al 1998). Physics of the so-called “advanced tokamak” and its prospects for steady-state operation have been recently reviewed (e.g. Taylor 1997, Gormezano 1998b, Litaudon 1998).

This paper reports the energy transport properties in Tore Supra and JET improved core confinement regimes for separately the electron and ion species. This work is motivated by two key issues for future application of such regimes in a fusion tokamak reactors. First, fusion core reactivity scales as approximately the square of the central ion pressure and therefore improved core confinement regimes aimed at reducing particle and ion thermal diffusivities to substantially increase fusion production. Second, improved electron confinement is of prime impor-

tance for sustaining thermonuclear burning plasmas since electron heating by fusion alpha-particles will be a dominant heating source.

The paper is divided in two main sections which describe recent experimental results and present understanding of the underlying physics of improved core confinement regimes obtained with dominant electron or ion auxiliary heating schemes. After this introduction, we present in section 2 the electron transport properties of discharges obtained in JET and Tore Supra when lower hybrid waves are applied at modest power (≈2MW) during the plasma current rise to form a broad current density profile. Reduction of electron thermal diffusivity observed in the plasma core is attributed to the formation of a weak central magnetic shear region. Section 3 is devoted to the JET optimised shear regime where ITBs are produced with a combination of high power (≥15MW) neutral beam injection (NBI) and ion cyclotron resonance heating (ICRH). Significant peaking of the profiles, indicative of an ITB, is observed in the electron density, toroidal rotation, ion and electron temperatures in plasma fuelled with pure deuterium (D-D) or a mixture of deuterium-tritium (D-T) ions (Gormezano et al 1998a). Emphasis is given in this paper on two new results : 1) ITBs have been produced in D-T plasmas with similar additional power levels to those in D-D, and 2) significant reduction of electron anomalous transport is obtained in addition to the well-known enhancement of ion energy content. After a brief description of the operational scenario, analyses focus on the characterisation of the energy transport in D-D and D-T plasmas. It will be shown that the combined role of magnetic shear and ExB velocity shear can explain the formation and evolution of a core region with reduced anomalous electron and ion heat transport. Finally, we conclude in section 4 and give perspective for future experiments.

2. IMPROVED CORE CONFINEMENT WITH DOMINANT ELECTRON HEATING SCHEME

This section is devoted to Tore Supra and JET experiments where similar spontaneous transitions to enhanced core electron confinement state have been observed during lower hybrid current drive (LHCD) experiments.

2.1. Scenario description and experimental results in JET and Tore Supra

In JET, LHCD is routinely used to assist the breakdown at the plasma formation and/or to preform the current density profiles when the current is ramped-up to produce “optimised shear” configuration (JET team 1997). Central electron temperature (T_{eo}) transitions to high values up to 10keV (volume averaged density, $\langle n_e \rangle \approx 0.8 \times 10^{19} m^{-3}$) are generally observed during the LHCD assisted ramp-up phase of the discharge even at modest applied power levels (2MW) (Ekedahl et al 1998). Typical time evolution of two discharges with similar plasma parameters are shown in Fig. 1 (left) where T_{eo} increases spontaneously at different times for different LHCD power ($t \approx 4.5s$ and $t \approx 3s$ respectively for the dashed and full line curves). Formation of a core region with a steep electron temperature gradient, indicative of enhanced electron confinement, is clearly

observed on the radial electron temperature profiles (Fig.1 (right)) [the ion temperature profile is not measured since the charge exchange diagnostic requires NBI power]. Broader T_e profiles are measured before transition to an improved core confinement phase as shown on the same figure.

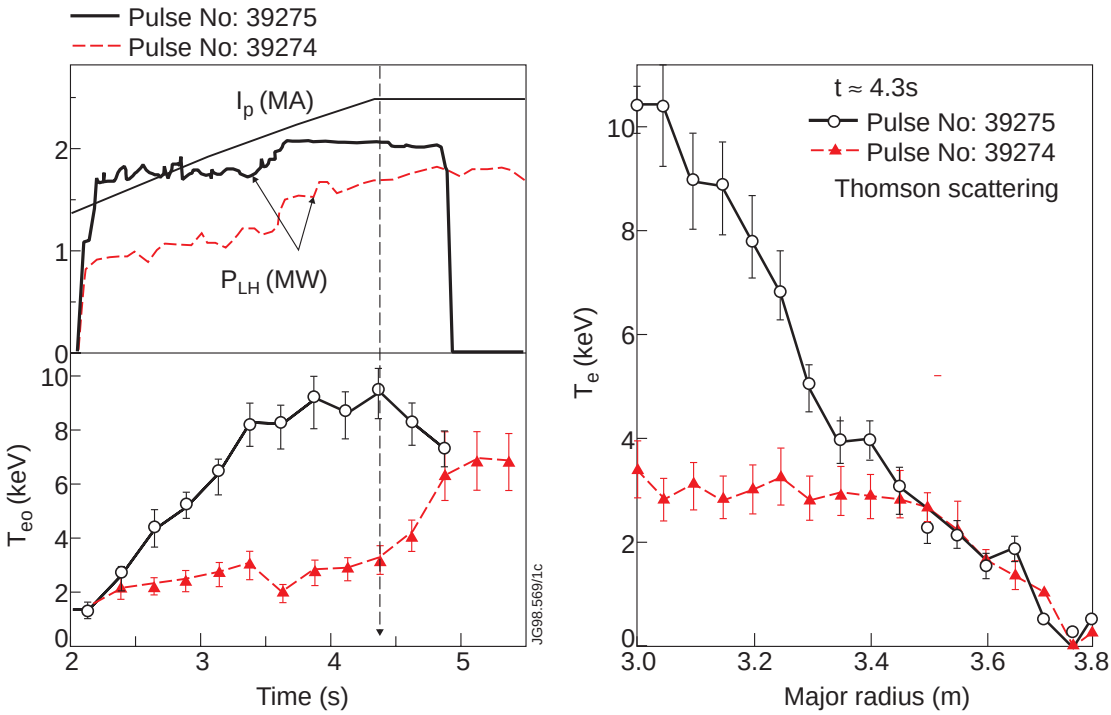

Figure 1. JET. (left) Time evolution of plasma current, LH power and central electron temperature for two LHCD-assisted current ramp-up discharges; (right) Electron temperature profiles for both discharges at t≈4.3s (Thomson scattering measurement). Full lines and dashed lines correspond respectively to Pulses N° 39275 & 39274.

In Tore Supra, transitions to enhanced core confinement were initially reported by similar spontaneous increases of T_{eo} in fully non-inductive LHCD discharges performed at reduced plasma density ($\langle n_e \rangle \approx 10^{19} m^{-3}$) with typically 3MW of power (Moreau et al 1993, Hoang et al 1994, Tore Supra Team 1996). The present experimental effort is devoted to optimise the route towards high density long-pulse operation by increasing the applied power and the bootstrap current fraction. A possible strategy to achieve this long term objective consists in forming a hollow current density profile already during the ramp-up phase (Joffrin et al 1998). For this purpose, technical activities have focused on the optimisation of the start-up of the discharge by controlling the fast and full expansion of the plasma cross-section just after the breakdown in order to maximise the edge current. In addition, LH waves are used in the early phase of the discharge to provide electron heating and slow down the resistive evolution of the current. The LH power waveform is adjusted in accordance with the plasma current ramp-up conditions. Using this operational procedure, weak or reversed magnetic shear configurations have been obtained in a reproducible manner even at high density and maintained for about one second. Direct evidence of the formation of an internal zone with a negative shear is shown on the time traces of the minimum (q_{min}) and on-axis (q_o) values of the safety factor, Fig. 2 (left). During

the reversed magnetic shear phase, improvement of the electron confinement in the plasma core is observed as an increase of the T_{eo} up to 4.5keV with only 1.6MW of LH power at $\langle n_e \rangle = 2.0 \times 10^{19} m^{-3}$. The q-profile determined by the magnetic reconstruction code IDENT-D shows that q_{min} is close to 2 at the magnetic surface r/a=0.45. The improved electron confinement concerns mainly the central part of the discharge where the magnetic shear is small.

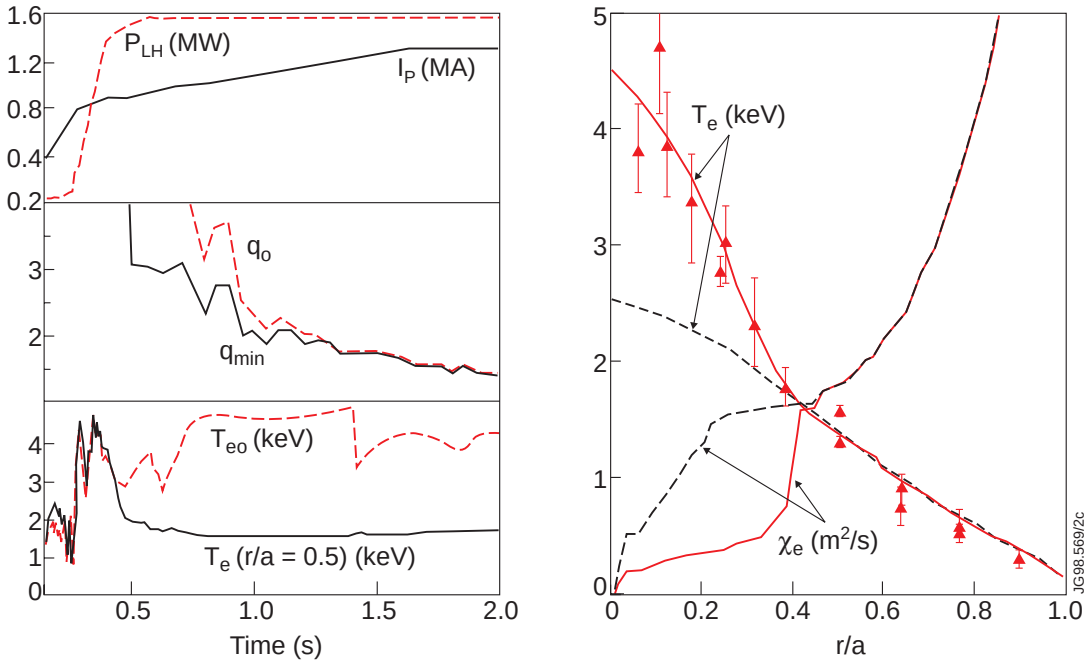

Figure 2. Tore Supra. (left) Time evolution of main parameters (LH power, plasma current, q_o, q_{min}, T_{eo} and T_e at r/a≈0.5) during LHCD-assisted current ramp-up; (right) Experimental (plain triangles) and simulated T_e profiles (full line) during the improved core confinement phase (t≤1.4s). The dashed line corresponds to a simulation performed without including the magnetic shear dependence in the transport model. The predictive χ_e are also shown. Pulse No 22650.

2.2. Predictive transport modelling of improved core electron confinement in Tore Supra

The mixed Bohm and gyro-Bohm transport model developed at JET (Erba et al 1997, Parail et al 1998a) has been used for the predictive heat transport simulations described in this subsection. This model has been successful in simulating a large range of L-mode or H-mode regimes in JET and in various tokamaks (ITER profile data base) (Erba et al 1998). It is natural to extend it to describe the formation of peaked electron temperature profiles observed during the current profile control experiments with LHCD.

The distinctive feature of this model is that it consists of a combination of a Bohm and gyro-Bohm type of anomalous transport. To link the electron thermal diffusivity (χ_e) to the magnetic shear, the Bohm term is cancelled in the region of zero or negative magnetic shear :

$$\chi_e = c_1 \chi_{Bohm} \left| \frac{\nabla p_e}{p_e} \right| q^2 \left| \frac{\nabla T_e}{T_e} \right|_{edge} \times H(s) + c_2 \rho^* \chi_{Bohm} \left| \frac{\nabla T_e}{T_e} \right| \qquad (1)$$

$$\text{where } H(s) = \begin{cases} 1 \text{ when } s = \dfrac{rdq}{qdr} > 0 \\ 0 \text{ when } s \le 0 \end{cases}$$

Here, $\chi_{Bohm} = T_e/B_T$ is the pure Bohm diffusivity, P_e is the electron pressure, q the safety factor, ρ^* the normalised Larmor radius in the toroidal magnetic field (B_T), and c_1-c_2 are fixed dimensionless coefficients. The pure Bohm and gyro-Bohm transport are amplified by strong edge losses described by the $q^2 \frac{\nabla P_e}{P_e}$ and $\frac{\nabla T_e}{T_e}$ terms (Erba et al 1997). A non-local dependence on the normalised temperature scale length at the plasma edge has been included in the Bohm term to simulate both L and H-mode regimes. The theoretical justification for explaining the magnetic shear effect on the anomalous thermal transport is well developed and based on the transition of the associated turbulence from a non-local (Bohm term) to a local character (gyro-Bohm term) when the magnetic shear decreases (e.g. Romanelli & Zonca 1993). In theory of anomalous transport due to global modes, reduction of transport in the low magnetic shear region is explained as a result of the toroidal decoupling of the modes, with a subsequent decrease of the radial correlation length of the fluctuations.

The transport model with the magnetic shear dependence is now applied to the recent current ramp-up experiments performed at higher plasma density in Tore Supra. The electron temperature profile is correctly simulated because the electron thermal transport coefficient is decreased down to the gyro-Bohm level inside r/a≈0.4 and a significant part of the LH power is deposited within this radius (Fig. 2(right)) (Erba et al 1998, Joffrin et al 1998). The LH power deposition profile is directly deduced from the fast electron bremsstrahlung tomography measurements (Peysson et al 1997, Imbeaux et al 1998). The predictive transport simulation of T_e profiles performed without including the magnetic shear dependence in the electron thermal diffusivity model is shown on the same figure (dashed line). A better agreement with the electron temperature measurement is obtained when χ_e is reduced close to the gyro-Bohm level only, in the weak magnetic shear region consistent with previous analyses (Litaudon et al 1997, Voitsekhovitch et al 1997).

3. INTERNAL TRANSPORT BARRIER WITH DOMINANT ION HEATING SCHEMES IN JET

High performance discharges with a central region of good confinement are produced in the so-called JET “optimised shear” regime with a combination of ICRH (≤6MW) and NBI (≤20MW) powers. Operational aspects are first described in this section, followed by analyses of energy transport in D-D and D-T optimised shear plasmas.

3.1. Optimised shear regime : operational scenarios in D-D and D-T plasmas

After a low voltage breakdown assisted by LHCD power, operational scenario consists in heating the plasma with a proper sequence of ICRH and NBI powers during the current rise phase of the discharge (Sips et al 1997). The current is usually ramped at a rate of 0.4MA/s with a lower single null X-point. Fundamental hydrogen minority heating scheme is used for ICRH with the

resonance near the plasma centre. Pressure and q-profiles are controlled during a pre-heating phase performed at reduced power level. This phase ends when high power is applied at low density : typically 18MW of NBI and 6MW of ICRH. Then a core region with steep pressure gradients can be formed in a variety of conditions depending on the power waveforms (time sequence and power level) and on the initial plasma profiles. High performance is achieved in D-D plasmas when ITBs are triggered just at the start of the main heating phase while keeping an L-mode edge as long as possible, i.e. the highest fusion yield in D-D plasmas in JET has been obtained in this way (Söldner et al 1997).

ITBs were not produced in D-T plasmas using exactly the same scenario as the one developed during the D-D preparation experiments. The two major reasons for these differences were the lower L to H mode power threshold in D-T plasmas (Jacquinot et al 1998) and different q-profiles at the start of the high power phase. The target q-profiles have q-values above one everywhere and it was empirically found that prompt ITBs are formed when the plasma volume inside the q=2 surface is sufficiently large (Gormezano 1998b). The q-profiles are determined from magnetic reconstruction and presence of q=2 surface is confirmed by m=2, n=1 MHD activity. Therefore, the power waveforms during the pre-heating phase were modified in order to avoid an early formation of an H-mode and to establish similar q-profile as in D-D plasmas just prior to the application of the high power. With such modifications, ITBs were successfully produced for the first time in D-T plasmas with similar additional heating power levels to those in D-D (Gormezano et al 1998a).

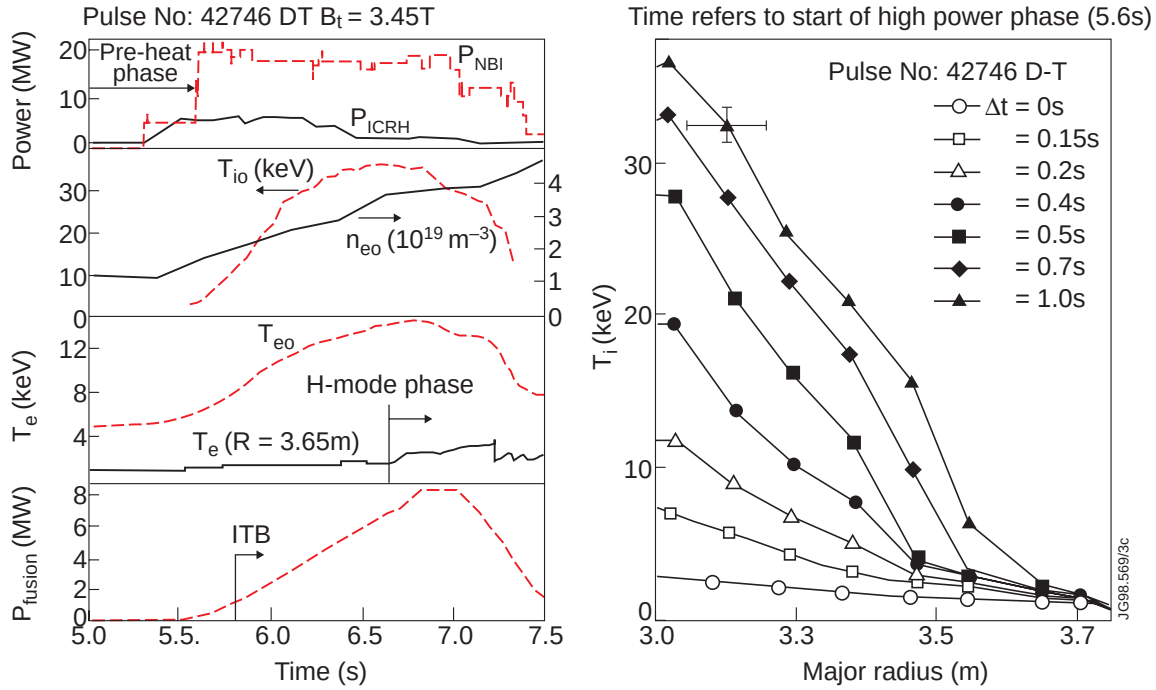

Figure 3. JET. Optimised shear scenario in D-T at B_t=3.45T. (left) Time evolution of applied power, central ion temperature, central electron density, central electron temperature and produced fusion power. The plasma current is increased at 0.4MA/s up to 3.24MA at t=7s. (right) Radial ion temperature profiles from charge exchange spectroscopy. An ITB is triggered 200 ms after the start of the high power phase. Pulse No 42746.

An example of a typical D-T discharge with prompt ITB formation is shown on Fig. 3 (left). Presence of an ITB is clearly revealed as large gradients in the ion temperature profiles are build-up (Fig. 3 (right)). After the ITB formation with peaked pressure profiles, on-axis ICRH heating is reduced in real-time to maintain a stable discharge close to the predicted ideal MHD stability boundary for kink-modes (Huysmans et al 1997). The phase with an L-mode edge lasts until time t=6.7s when transition to an ELM-free H-mode occurs. Subsequently, several large ELMs terminate the phase of the improved confinement. This sequence of events is very similar to that in D-D except that the duration of the L-mode edge phase, during which the central density builds-up, is shorter in D-T probably as a result of the lower L to H-mode power threshold. At the peaked performance, up to 8.2MW of fusion power were produced at $n_{eo} \approx 3.8 10^{19} m^{-3}$, $T_{io} \approx 32$keV, $T_{eo} \approx 14$keV and with an estimated tritium concentration of about 30% (cf. table 1).

Table 1. *JET. Parameters for a high fusion power D-T optimised shear pulse (No 42746) at t= 6.82s (cf. Fig. 3).*

Plasma current :	3.2 MA
Magnetic field :	3.45T
Plasma major radius :	2.9m
Plasma minor radius :	0.9m
ICRH power :	2MW
NBI power :	18MW
Ohmic power :	0.2MW
Alpha power :	1.6MW
Fusion power :	8.0 ±10%
Central electron density :	$3.8 10^{19} m^{-3}$
Central Deuterium and Tritium density :	$2.9 10^{19} m^{-3}$
Central electron temperature :	14keV
Central ion temperature :	32keV
Central toroidal rotation :	38.9kHz
Central Tritium concentration :	0.29
Central effective charge (Z_{eff}) :	1.3
Diamagnetic stored energy :	11MJ
Normalised toroidal beta (β_N) :	1.75
Energy confinement time :	1.1s
Energy confinement time normalised to ITER89 scaling:	2.9

An approach to sustain high fusion yield production consists in the combination of an ITB with a weak edge pressure pedestal of the ELM'y H-mode. In D-D plasmas, the optimised shear regime was sustained during 4 confinement times (≈2s) with an ELM'y H-mode (Söldner et al 1997). In D-T plasmas, this operation mode was easily reproduced due to the reduced power threshold for the L to H-mode transition and up to 7.0MW of fusion power was produced (Fig. 4) (Söldner et al 1998). This approach has not been exploited during the 1997 D-T experimental campaign : the input power was deliberately stepped down one second after the high power phase to minimise the production of 14MeV neutrons. Nevertheless, these are promising results for future steady-state operation with X-point magnetic configurations since the edge transport barrier is sufficient to broaden the total pressure while regular ELMs avoid a continuous build-up of current and pressure at the edge which usually lead to the disruptive termination of the ELM-free H-mode phase.

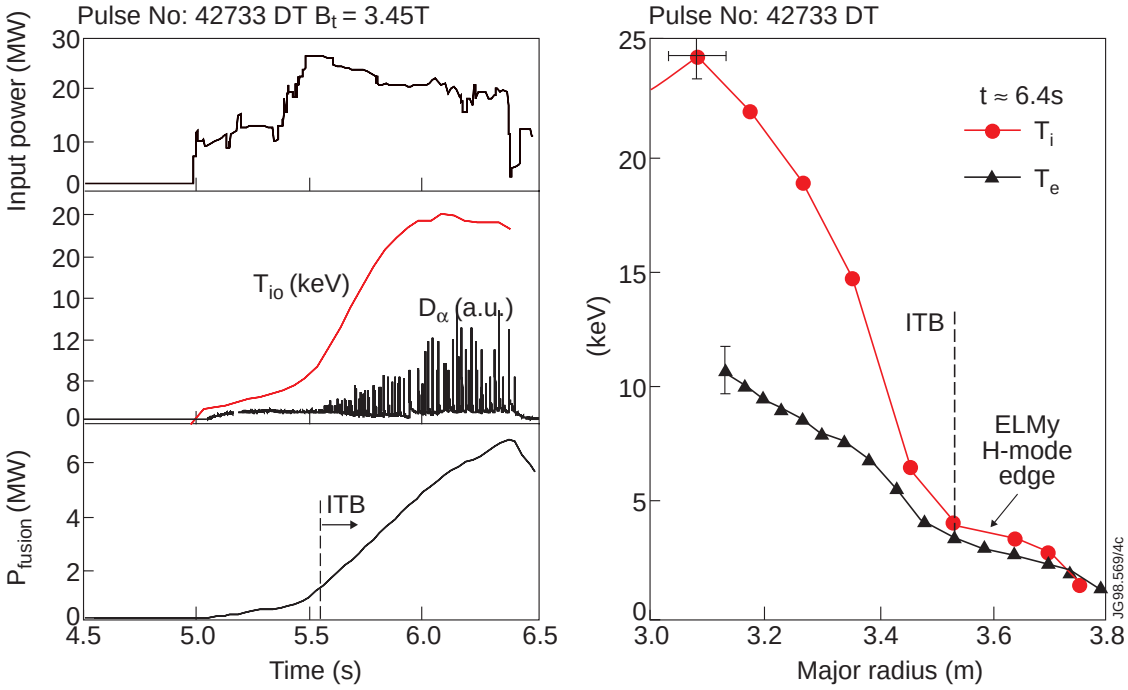

Figure 4. JET. ITBs sustain with an ELMy H-mode edge in D-T at B_t=3.45T. (left) Time evolution of total applied power during the high performance D-T phase, central ion temperature, D_α and fusion power. (right) Radial ion temperature profiles from charge exchange spectroscopy and electron temperature profile (ECE measurement) at t=6.4s. Pulse No 42733.

3.2. Energy transport in D-D and D-T optimised shear plasmas

Presence of an ITB is clearly revealed as a large reduction of the ion thermal diffusivity, χ_i, inside the central region. In pure deuterium discharges, local transport analyses with TRANSP show a reduction of χ_i to 0.1-0.2m^2/s comparable to its standard neoclassical level (Cottrell et al 1998a). Ion thermal diffusivities drop to similar levels in D-T discharges when ITBs are produced with identical input powers and q-profiles to those in D-D (Gormezano et al 1998) (Fig. 5). The region of good confinement with steep gradients in the ion temperature profile is

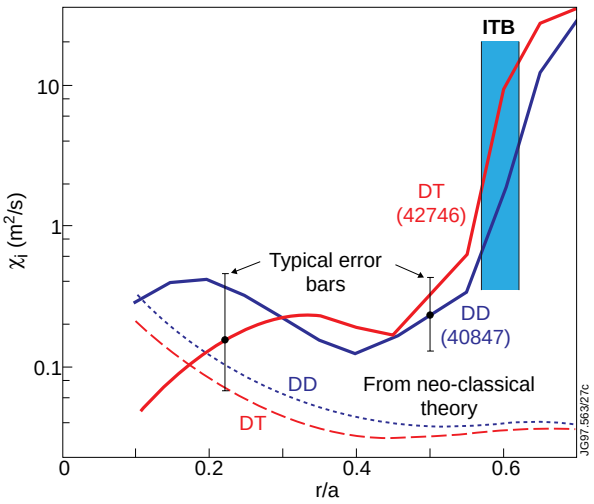

Figure 5. JET. Radial ion thermal diffusivity profiles in D-T and in D-D for a similar reference case at 1s after the pre-heating phase. Pulse No 42746 (D-T) and 40847 (D-D).

formed close to the magnetic axis and expands outwards to approximately 2/3 of the plasma radius. After the expansion process, χ_i is reduced everywhere inside the core region.

Formation of steep gradients in the electron temperature profile (inside R<3.65m) is also observed for both D-D and D-T plasmas (Fig. 6). Radial T_e profiles are measured with the electron cyclotron emission diagnostic using an heterodyne radiometer technique and has small spacial resolution of ±0.03m. Location of the transition from a high to a low transport region is determinated from the position of the maximum of the second radial derivative of the ion and electron temperature profiles. The calculation has been performed for a large variety of optimised shear discharges in D-D and D-T plasmas. From the results shown in Fig. 7 we conclude that the development of steep temperature gradients follows the same time evolution (i.e. formation, expansion and contraction) at the same radial location for both the ions and electron components.

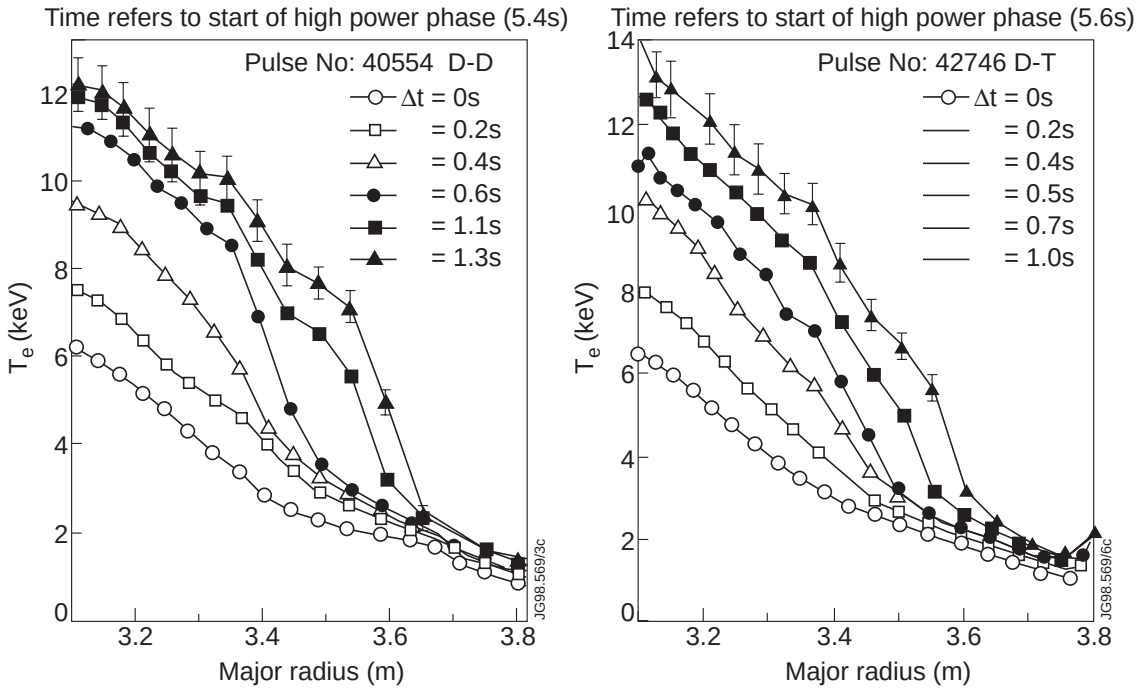

Figure 6. JET. (left) Radial electron temperature profiles at different time after the high power phase in D-D (40554) and (right) in D-T (Pulse No 42746) showing the formation of an electron ITB with an L-mode edge. T_e is measured with the ECE heterodyne radiometer diagnostic.

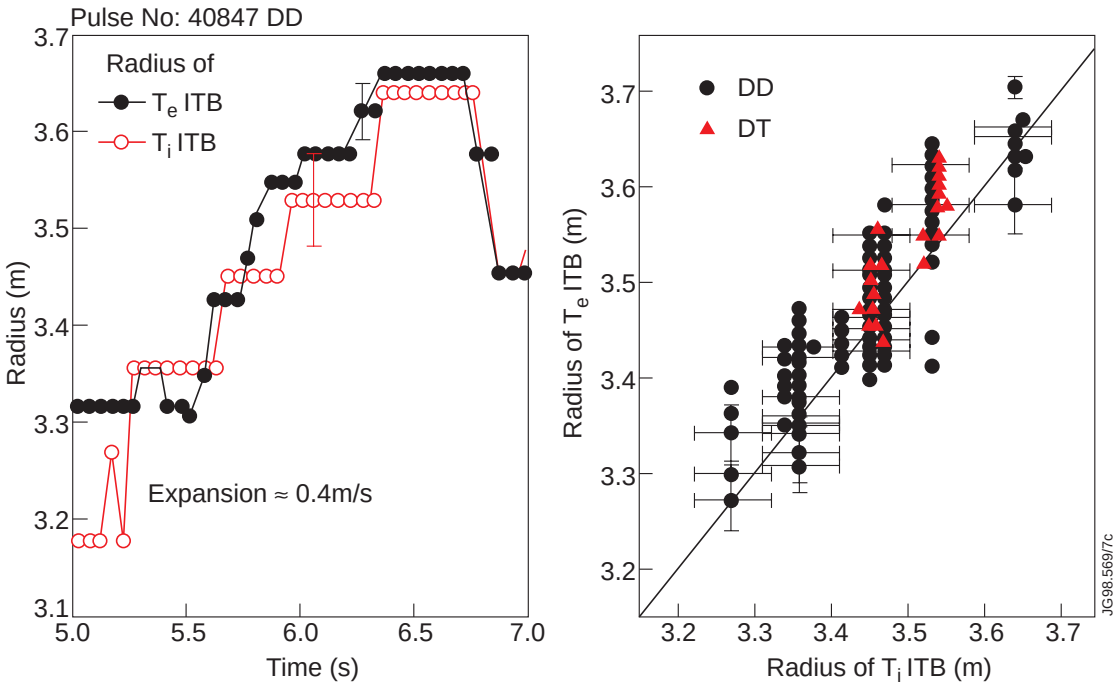

Figure 7. JET. (left) Time evolution of radial location of both the ion and electron ITB. Pulse No 40847 (D-D). (right) Radial location of the electron ITB versus the radial location of the ion ITB for a large number of D-D (plain circles) and D-T (plain triangles) pulses. The charge exchange spectroscopy and ECE measurements have been used for respectively the ion and electron profiles.

Formation of peaked T_e profiles is indicative of a reduction of the anomalous electron transport which is now assessed in both global and local confinement analyses. In the first study, the central electron pressure is plotted versus the total power flowing into the electron channel, i.e. the sum of the ICRH and NBI powers deposited on electrons, ohmic and equipartition electron heating (Fig. 8 (left)). This sum is corrected by the power lost in changing the electron thermal energy content (W_e), i.e. dW_e/dt. Each quantity has been obtained from TRANSP calculations where the total energy content and neutron rate of the experiments are well reproduced by the code calculations. The RF power deposited on the electrons includes both the direct wave absorption on thermal electron (through transit time magnetic pumping and electron Landau damping) and the redistributed power to electrons from the minorities species. As described by Cottrell et al (1998b), the ICRH computations in TRANSP have been found in good agreement with the independent PION code for modelling ICRH (Eriksson et al 1993). A clear signature of a transition into a state with enhanced electron confinement is shown in Fig. 8(left) : the central electron pressure is approximately five time higher in the optimised shear regime compared to a standard heating case at the same power. The second study consists in local interpretative transport analyses where the electron temperature (from ECE measurements) is given as a function of frequency and then mapped, self-consistently, on to the radial space co-ordinate using the TRANSP equilibrium solver. Characteristic radial profiles of the electron thermal diffusivities from TRANSP are shown on Fig. 8 (right) for a D-T pulse. When the high power (≈25MW) is applied χ_e is of the order of $5m^2/s$ in the confinement zone (i.e. at normalised minor radius, r/

a≈0.6), and decreases by a factor 16 down to 0.3m^2/s after the transition into an improved confinement state. It is worth mentioning that χ_e rises to a level of 1m^2/s inside the region between r/a≈0.2 and r/a≈0.4 which is attributed to local MHD phenomenon deteriorating the electron confinement (Baranov et al 1998).

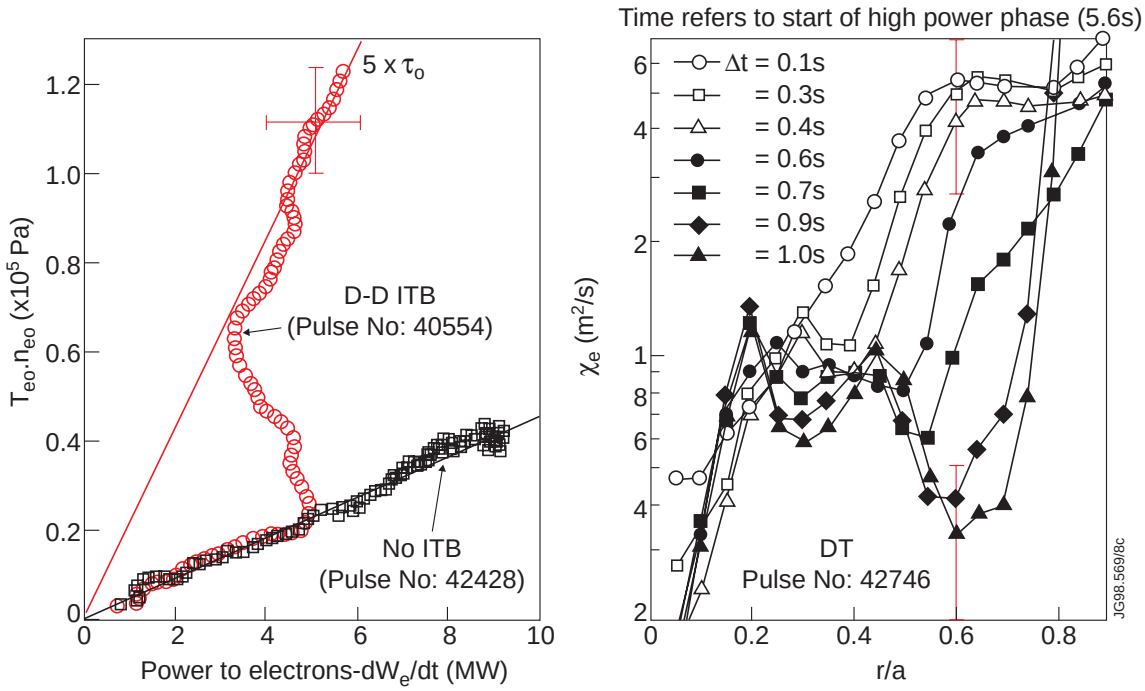

Figure 8. JET. (left) Central electron pressure versus the power transferred into the electron channel corrected by the time variation of the electron energy content for D-D pulses (L-mode edge). (right) radial electron thermal diffusivity profiles from TRANSP in D-T at different time during the high power L-mode phase for the pulse shown in Fig. 3. Pulse No 42746.

For the same discharge, the electron diffusivities (at r/a≈0.6) have been plotted versus the local electron temperature gradient (∇T_e), i.e. the source of free energy in the plasma which may drive the anomalous electron transport (Fig. 9 (left)). Before the barrier formation, a standard L-mode confinement branch is followed where χ_e increases linearly with ∇T_e (i.e. degradation of confinement with additional input power). Then, χ_e values decrease by following an other branch where a reduced anomalous transport state is reached with ∇T_e up to 35keV/m. For comparison, the Bohm and gyro-Bohm electron transport coefficients (defined in equation one) have been plotted in the same diagram. The experimental χ_e values drop below the anomalous gyro-Bohm level which was successfully used to quantify the core electron confinement improvement described in section 2. We complete this comparison by analysing the phase of the discharges where ITBs are sustained with the ELM-free H-mode regime, i.e. with edge transport properties mainly described by the gyro-Bohm dependence (Parail et al 1998a). The remarkable feature of this phase is that steep electron temperature gradients are observed inside the plasma core in addition to the temperature pedestal at the plasma edge. Indeed, local transport analyses with TRANSP indicate that χ_e is below 1.4m^2/s over the entire plasma cross section and sharply decrease down to 0.3m^2/s at the location of the internal barrier (Fig. 9 (right)).

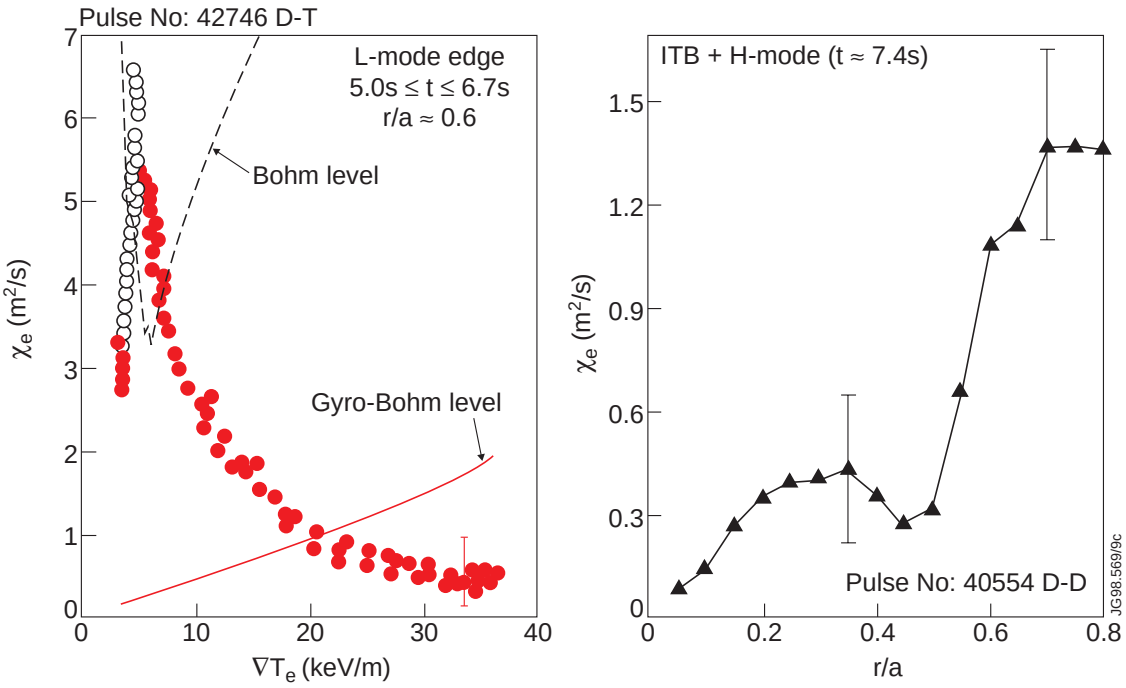

Figure 9. JET. (left) Electron thermal diffusivity at r/a≈0.6 versus the electron temperature gradient at the same location. Dashed and full lines correspond respectively to the anomalous Bohm and gyro-Bohm electron transport coefficients defined in equation 1. Pulse No 42746 (D-T). (right) Radial electron thermal diffusivity profiles from TRANSP during the ELM free H-mode phase. Pulse No 40554 (D-D).

3.3. Predictive transport modelling of JET optimised shear discharges

The interplay between the magnetic shear and ExB velocity shear has been investigated in the predictive transport simulation of the ion temperature profiles using the mixed Bohm/gyro-Bohm model (Parail et al 1998a,b). The enhanced confinement in the core is formed by decreasing the dominant Bohm ion thermal diffusivities down to a combination of gyro-Bohm and neoclassical terms. When taking into account only the effect of the weak magnetic shear to cancel the Bohm coefficient as described in section 3.3, ITB could not be reproduced (fig. 10 (left)). The effects of ExB velocity shear on the growth rates and radial extent of turbulence eddies in the plasmas have to be considered in the formation and development of ITBs. As reviewed by Burrell (1997) and Synakowski (1998), ExB velocity shear can lead to transport reduction through the decorrelation of fluctuations and stabilisation of the unstable modes. But self-consistent simulations which rely only on the ion pressure gradient term in the radial electric field equation, produce a too wide region with reduced transport coefficients (fig. 10 (left)). Indeed, formation of steep ion pressure gradients increases the ExB velocity shear which reduces the anomalous transport in a wider region and then reinforce the pressure gradients. Absence of stabilising term in the positive feedback loop between ion pressure gradients and ExB velocity shear leads in the predictive transport modelling to an almost instant propagation of the transport barrier across the entire plasma cross section. Simulations which give a reasonable agreement with the experimental data take into account the combined role of the magnetic and

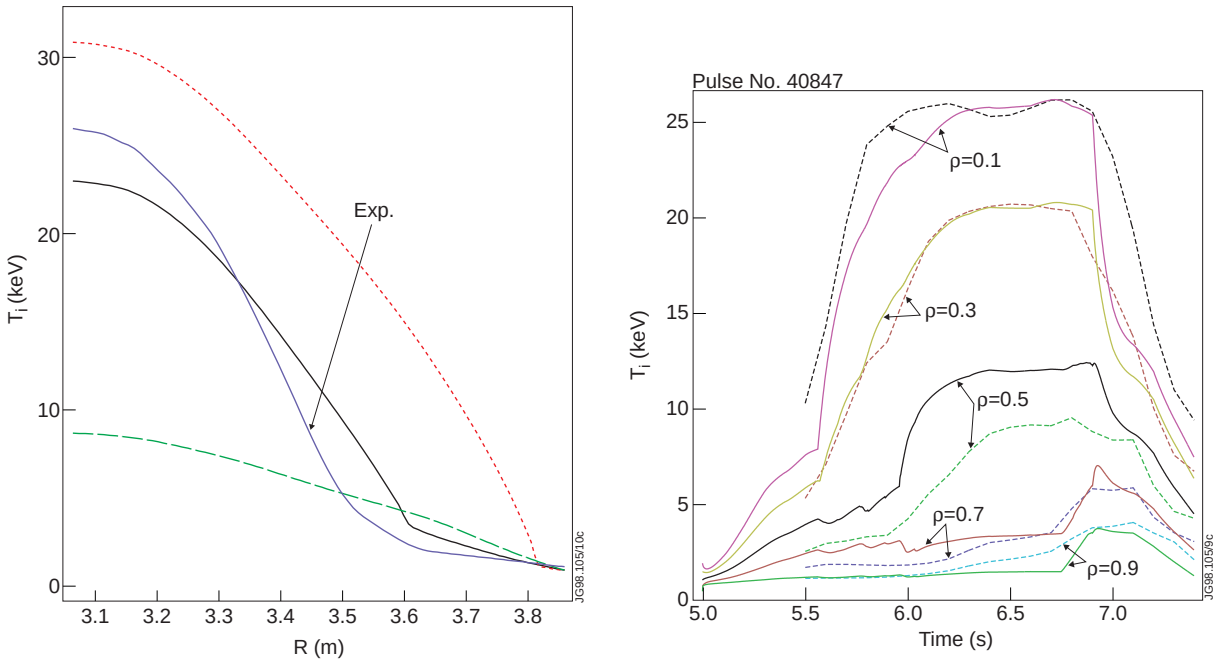

Figure 10. JET. Transport modelling of the ion ITB. (left) Experimental and simulated radial ion temperature profiles. The thick full line corresponds to a simulation performed taking into account the combined role of magnetic and ExB shear in the transport model. Simulations performed with only the magnetic shear (large dash) or only the ExB shear (small dash) dependence are shown for comparison. (right) Experimental (dashed line) and simulated (full line) time evolution of the ion temperature for different radial location showing the formation and evolution of the ion ITB. The simulation is performed taking into account the combined role of magnetic and ExB shear in the transport model. Pulse No 40847 (D-D).

ExB velocity shear. The Bohm term is cancelled when the ExB shearing rate normalised to the maximum linear growth rate of drift type plasma turbulence exceeds the local magnetic shear value (Parail et al 1998b). Therefore, the radial expansion process is stabilised in a region where the ExB velocity shear could not overcome the positive magnetic shear. As shown on Fig. 10 (right), this approach allows to reproduce the main features of the ion temperature evolution.

4. SUMMARY OF PROGRESS AND PROSPECTS

Core regions with reduced transport coefficients have been obtained both in Tore Supra and JET by heating the plasma during the current rise phase of the discharge. Characteristics of the good confinement regions and the physics process involved in their formation and maintenance should be considered separately when the electron or ion components are predominantly heated.

With a dominant electron heating scheme (LHCD), improved electron confinement in the plasma core is obtained in Tore Supra and JET at low power levels (2MW) with an L-mode edge. In these discharges, no sign of power threshold and rapid radial expansion of the improved confinement zone are reported. The weak or reversed magnetic shear configuration plays a major role in reducing the electron anomalous transport coefficients from a Bohm term down to a gyro-Bohm level.

In JET optimised shear regime with dominant ion heating schemes (NBI and ICRH), significant reduction of the energy transport is obtained for both the electron and ion components during the high power phase (≥15MW). Formation of ITBs is successfully achieved in a fuel mixture of deuterium and tritium and fusion power of up to 8.2MW is produced in this regime. ITBs have been produced in D-T plasmas with similar additional heating power and similar plasma current to those in D-D. Ion thermal diffusivities are comparable to neo-classical levels and electron thermal diffusivities decrease by one order of magnitude at mid-plasma radius in both D-D and D-T plasmas. The good confinement region is formed close to the magnetic axis and expands radially with time. Transition between an high and low transport region occurs at the same radial location for both the electron and ion components. These results underline a common physics process to reduce the electron and ion energy transport. Finally, transport modelling of these experiments require to invoke the combined turbulence reduction mechanisms of the magnetic and ExB velocity shears to reproduce the formation and development of the ITBs.

Results presented in this paper are promising for future fusion tokamak reactors with internal transport barriers, i.e. i) establishment of ITB with different fuel mixtures (D-D and D-T) with similar applied power, ii) enhanced electron and ion confinement, iii) influence of the current profile to extend and ultimately control the radial location of the ITB, iv) coexistence of two transport barriers in the plasma edge and in the core to control pressure and bootstrap current profiles. Nevertheless, several aspects should be explored to extrapolate with better confidence this recent operating mode to fusion tokamak reactors, e.g. i) determination of the power threshold dependence with the machine size or plasma parameters, ii) maintaining ITBs with mostly electron heating and low particle fuelling rates in the core as expected in a burning plasma, iii) development of integrated plasma control of pressure and q-profiles (Moreau et al 1998). Important part of the future experimental campaign planned at Tore Supra and JET will focus on these issues.

ACKNOWLEDGEMENTS

The authors are grateful to A. Taroni and E.M. Springmann for useful discussions and use of the transport code JETTO. It is a pleasure to acknowledge the entire Tore Supra and JET teams.

REFERENCES

Baranov Yu. et al 1998 submitted to Nucl. Fusion.

Bécoulet A., Basiuk, V., Hoang G.T., Joffrin E. 1998 Plasma Phys. Control. Fusion **40** to be published.

Burrell K. H. 1997 Phys. Plasmas **4** 1499.

Cottrell G.A. et al 1998a Plasma Phys. Control. Fusion to be published.

Cottrell G.A. et al 1998b submitted to Nucl. Fusion.

Ekedahl A. et al 1998 to be published in Nucl. Fusion.

Equipe Tore Supra 1996 Plasma Phys. Control. Fusion **38** A251.

Erba M., Cherubini A., Parail V., Sprigmann E. and Taroni A. 1997 Plasma Phys. Control. Fusion **39** 261.
Erba M. et al 1998 proceedings of this conference.
Eriksson L.G., Hellsten T., Willén U. 1993 Nucl. Fusion **33** 1037.
Gormezano C. et al 1998a Phys. Rev. Letters **80** 5544.
Gormezano C. 1998b Plasma Phys. Control. Fusion **40** to be published.
Hoang G.T. et al. 1994 Nucl. Fusion **34** 75.
Huysmans G. et al 1997 Controlled Fusion and Plasma Physics (Proc. 24th Eur. Conf. Berchtesgaden 1997) vol. 21A (Geneva: EPS) p 21.
Ishida S. et al 1997 Phys. Rev. Letters **79** 3917.
Imbeaux F., Peysson Y., Joffrin E. and Litaudon X. 1998 Controlled Fusion and Plasma Physics (Proc. 2nd Top. Conf. on RF heating, Brussels, 1998) vol XXA (Geneva: EPS) pXX.
Jacquinot J., Bhatnagar V.P., Gormezano C. et al 1993 Plasma Phys. Control. Fusion **35** A35.
Jacquinot J. et al 1998 this issue of Plasma Phys. Control. Fusion.
JET Team 1997 Plasma Physics and Controlled Nuclear Fusion Research (Proc. 16th Int. Conf. Montreal 1996) vol. 1 (Vienna: IAEA) p 487.
Joffrin E. et al 1998 proceedings of this conference.
Kikuchi M. 1990 Nucl. Fusion **30** 265.
Levinton F.M.et al 1995 Phys. Rev. Lett.**75** 4417.
Litaudon X. et al 1997 Plasma Physics and Controlled Nuclear Fusion Research (Proc. 16th Int. Conf. Montreal 1996) vol. 1 (Vienna: IAEA) p 669.
Litaudon X. 1998 Plasma Phys. Control. Fusion **40** A251.
Parail V. et al 1998 Plasma Phys. Control. Fusion **40** 805.
Parail V. et al 1998 submitted to Nucl. Fusion.
Peysson Y., Delpech L., Imbeaux F., Litaudon X. and Sébelin E. 1997, Controlled Fusion and Plasma Physics (Proc. 24th Eur. Conf. Berchtesgaden, 1997) vol 21A (Geneva: EPS) p229.
Moreau D. et al. 1993 Plasma Physics and controlled Nuclear Fusion Research (Proc. of 14th Int. Conf. Würzburg 1992) Vol. 1 (Vienna: IAEA) p 649.
Moreau D., Voitsekhovitch I. et al. proceedings of this conference.
Romanelli F. and Zonca F. 1993 Phys. Fluids B**5** 4081.
Sips A. et al 1998 Plasma Phys. Control. Fusion **40** 1171.
Synakowski E. 1998 Plasma Phys. Control. Fusion **40** 581.
Söldner F.X. et al. 1997 Plasma Phys. Control. Fusion **39** B353.
Söldner F.X. et al. 1998 submitted to Nucl. Fusion.
Strait E.J. et al. 1995 Phys. Rev. Lett. **75** 4421.
Taylor T.S. 1997 Plasma Phys. Control. Fusion **39** B47.
Voitsekhovitch I., Litaudon X., Moreau D. et al 1997 Nucl. Fusion **37** 1715.
Wagner F. et al 1982 Phys. Rev. Lett. **49** 1408.